STATISTICAL TECHNIQUES FOR THE IDENTIFICATION OF REACTOR COMPONENT STRUCTURAL VIBRATIONS

L.G. KEMENY

School of Nuclear Engineering,
University of New South Wales, Kensington, New South Wales, 2033, Australia

SUMMARY

The identification, on-line and in near real-time, of the vibration frequencies, modes and amplitudes of selected key reactor structural components and the visual monitoring of these phenomena by nuclear power plant operating staff will serve to further the safety and control philosophy of nuclear systems and lead to design optimisation. The rapid recognition of the onset of unusual or accidental conditions in reactor sub-channels by means of the optimal filtering of noise-like signals generated by vibrational and pressure fields and other correlated noise sources will lead to the development of new safety systems.

The School of Nuclear Engineering has developed a data acquisition system for vibration detection and identification. The system is interfaced with the HIFAR research reactor of the Australian Atomic Energy Commission. The reactor serves to simulate noise and vibrational phenomena which might be pertinent in power reactor situations. The data acquisition system consists of a small computer interfaced with a digital correlator and a Fourier transform unit. An incremental tape recorder is utilised as a backing store and as a means of communication with other computers. A small analogue computer and an analogue statistical analyzer can be used in the pre and post computational analysis of signals which are received from neutron and gamma detectors, thermocouples, accelerometers, hydrophones and strain gauges.

Investigations carried out to date include a study of the role of local and global pressure fields due to turbulence in coolant flow and pump impeller induced perturbations on (a) control absorbers, (b) fuel element and (c) coolant external circuit and core tank structure component vibrations. Resonant frequencies have been isolated within the range 0.5 Hz to 6.3 kHz. The effects of such resonances on the overall reactor transfer function have been assessed. New algorithms based on spectral optimisation and optimal filtering are undergoing development to identify transitions from normal to abnormal operating conditions. A technique for monitoring structural motion by neutron counting has been successfully tested.

1. Introduction

The SNEDAC System, Figure 1, is a multichannel, computer compatible data processor and analyzer for both analog and digital input signals. The system is itself equipped with limited computing capability. Alternatively it can be linked, on-line, to digital or analog computers or the acquired data may be transferred for analysis to a large digital computer through the medium of magnetic tape. The present system consists of five cabinets of electronic hardware, each of which may be used separately or as an interconnected, synchronisable unit. The designation of the five cabinets is as follows:

(1) Ancillary storage and recording equipment consisting of FM/DR instrumentation tape recorder, ultraviolet galvanometer recorder and chart recorder.

(2) Transducers and signal conditioning equipment and power supplies.

(3) Slow speed data logger to scan twenty channels at speeds up to 15 Hz with both paper tape and decimal print output.

(4) High speed digital data acquisition unit for dynamic and impulse response testing. This unit contains scalers, a digital pseudo-random noise generator with provision made for an on-line correlator.

(5) Computing section equipped with PDP8/L computer and a Precision Instruments tape recorder. This unit also contains fast analog to digital converters and has been equipped with a hard wired correlator with its own Fourier transform unit to provide two channels for very fast data analysis.

Signal flow is possible between each of the above cabinets and the addressing and scheduling of the operation of each of the transducer channels is under the control of the computer. At the present time the computer provides a limited arithmetical capability and all time consuming calculations have to be carried out off-line on an IBM 360/50 installation. Communication with the large computer is presently by means of the incremental tape deck. At a later stage a direct data link will be established between the two computers, using telephone cables. The future addition of 8K core store and a large disk will enable the SNEDAC system to utilise a Fortran, real time operating system.

SNEDAC is primarily designed for data collection in the general fields of neutron physics and nuclear science and engineering. Hence it is equipped to accept a large range of signal input levels and frequencies. Input transducers can be linked to electrometers capable of accepting microvolts. High level signals can be processed through a precision digital voltmeter. Between these extremes a number of other options are provided so that only in special cases is it necessary for the user to supply signal conditioning electronics. The frequency response of the data channels ranges from 100 Hz to 250,000 Hz and is planned to be adequate for a series of operations extending from slow speed scanning to high speed time correlation techniques.

The slow speed data logger consists of a precision digital voltmeter which provides analog to digital conversion, a one hundred point reed relay scanner, a high speed decimal printer and a paper tape punch.

The high speed digital data logger consists of 13 bit and 8 bit data channels with operational speeds up to 30 kHz. Direct in-core data flow at much higher speeds is also envisaged. A nine channel incremental tape recorder provides a backing store for large quantities of data and because of formatting arrangements also makes the SNEDAC system com-

patible with larger computers. For purposes of time series analysis an overall accuracy in measurement and data processing of 1% is obtainable. Playback from the tape is possible for monitoring purposes. The high speed system has three functions:

(a) On-line recording of experimental data followed by off-line analysis.

(b) On-line recording of experimental data accompanied by analysis for diagnostic and monitoring purposes.

(c) On-line recording of experimental data followed by analysis with the production of feedback signals for control and optimization purposes.

2. Stochastic Identification Techniques

The normal operation of nuclear power plant is characterized by a series of correlated vibrations or fluctuations ranging from flow induced structural vibrations to fluctuations in the neutron or gamma photon population density. The identification in the time or frequency domain of the time constants or resonant frequencies associated with these fluctuations gives rise to elegant power plant monitoring and control techniques. The forecasting or prediction of the state vectors associated with such fluctuations can, in principle, be used as a basis for emergency procedures associated with potentially abnormal operating conditions.

A simple Langevin model [1] for a stochastic system is given in Appendix 1. The basic identification, time series analysis and prediction techniques used in this investigation are given in Appendices 2, 3 and 4. The time series analysis programme is designed to compute multiple cross-correlation and cross-spectral density functions for up to eight stochastic variates. In fact, much of the present investigation is restricted to two channel cross-correlation. The data acquisition system will, on the basis of a scanning operation, record up to twenty channels of fluctuating signals. Such signals will normally be grouped into one or other of four categories

(1) Neutron and gamma photon density

(2) Mechanical vibration

(3) Hydraulic pressure fluctuation

(4) Metal or fluid temperature fluctuation

The constraints on the experimental measurements are set by the transducer employed; by the bandwidth of the data processing equipment, and by the sophistication of the mathematical algorithms used for analysis or control. Some features of the experimental apparatus are detailed below

TRANSDUCERS	Neutron and gamma ion chambers Proportional and fission counters Self powered neutron detectors Accelerometers, hydrophones, strain gauges, thermometers, ultrasonic transmitters and receivers.
DATA ACQUISITION BANDWIDTH	DC to 250,000 Hz for stochastic variates neutron, gamma and fission product number-density; temperature and pressure.
DATA ANALYSIS	All time series operations up to the multiple cross-correlation of eight stochastic variates, Identification and control algorithms.

Stochastic identification takes place subsequently to data recording and is applied to three areas of reactor system investigation as follows

NOISE SOURCE IDENTIFICATION	Time series analysis Probability density analysis Fourier and Walsh transforms Zero crossing analysis
REACTOR CORE, SYSTEM COMPONENT AND COOLANT CHANNEL IDENTIFICATION	Cross-covariance analysis Optimal filtering Optimal impulse response technique Integral equation and Green's function techniques
NOISE SIGNAL ANALYSIS FOR CONTROL AND PREDICTION	Variance minimisation Spectral optimisation Sampled data and z transform Convolution transform Linear, non-linear, stationary and non-stationary prediction techniques

The optimal prediction algorithm [2] utilizes the time series measurement of typical stochastic variates such as neutron density vibration and temperature to compute the conditional mean of a state vector $\underline{\xi}(t)$ when we have access to a measured time history $\bar{\mu}(t)$ in the range to $\leq T \leq t$. Here $\bar{\mu}(t)$ is an n dimensional measurement vector. For a typical power reactor system $\bar{\xi}$ and $\bar{\mu}$ may be related through reactor dynamic equations such as

$$\frac{d\bar{\xi}}{dt} = \alpha\bar{\xi} \quad \beta\bar{y} + \gamma\bar{z} \qquad \ldots(1)$$

and

$$\bar{\mu} = \Delta\bar{\xi} + \bar{\varepsilon} \qquad \ldots(2)$$

where $\bar{y}$ is a multi-dimensional input of known structure; $\bar{\varepsilon}$ is a multi-dimensional noise source with zero mean and $\bar{z}$ is a multi-dimensional noise source with zero mean.

The optimal estimate for $\bar{\xi}(t)$ can now be obtained by digital or analogue computer through the solution of an equation of the form

$$\frac{d\hat{\xi}}{dt} = \alpha\hat{\xi} + \beta\bar{y} + \eta(\bar{\mu}-\Delta\hat{\xi}) \qquad \ldots(3)$$

where α, β, γ and η are compatible matrices defined for the reactor system being identified. In essence the vector $\hat{\xi}(t)$ minimizes any convex function of the error

$$\tilde{\xi}(t) = \bar{\xi}(t) - \hat{\xi}(t) \qquad \ldots(4)$$

3. Experimental Results

Experimental results obtained to date are of an exploratory and tentative nature and high-light the gap which exists between sophisticated theory for simple, idealised vibrational models and the complex coupled system which is the reactor core structure.

Typical resonances which have been identified in both the time and frequency domain in HIFAR can be summarised as follows

PHENOMENON	RESONANT FREQUENCIES
EXTERNAL STRUCTURE BORNE AND SEISMIC VIBRATION INCLUDING CONFINEMENT AIRCONDITIONER	0.5 H_z 3 H_z 6 H_z
HYDROELASTIC VIBRATION OF FUEL ELEMENTS DUE TO PUMPING AND TURBULENT FLOW EFFECTS	10 H_z 800 H_z 6300H_z
REACTIVITY COUPLED VIBRATION OF CONTROL SYSTEM [Peak Vibration up to 3% of Mean Power]	6.5 H_z

The measurements were made with ion chambers, accelerometers and hydrophones to an overall accuracy of 5% which includes statistical uncertainty. The two most significant conclusions resulting from these preliminary measurements can be summarized as follows:

(1) Ion chamber and other neutron or gamma current cross-correlation techniques are capable of detecting and identifying the vibrational movement of control systems, fuel elements and core structure.

(2) The recording, storage and recall of spectral and impulse response patterns utilizing on-line computing equipment is a practical task and will undoubtedly become a standard diagnostic procedure in nuclear power plants of the future.

Some experimental results are shown in Figures 2 to 5. The neutron noise signals used in two detector cross correlation identification is shown in Figure 2. The emergence of a control absorber vibration as computed from such signals is shown in Figure 3. The hydroelastic responses of a dummy fuel element as measured with hydrophones and demonstrating both far and near field effects is shown in Figure 4. Vibrational patterns which may be stored, referenced and inspected are shown in Figure 5. Such patterns may range from simple acceleration levels on individual fuel elements (right hand side) to complete records of spectral density peaks (left hand side). The latter case [3] illustrates the emergence of a potential malfunction as clearances in a dummy fuel element increase and a fuel plate commences to vibrate.

4. Mathematical Modelling

The correlation of such experimentally observed phenomena with theoretical models is a difficult task because, unlike measurements in carefully controlled laboratory conditions, the transducer positions in a nuclear plant may not be optimally located. In the theoretical modelling of hydorelastic vibration phenomena, two approaches are possible. For simple geometries and in carefully planned measurements a rigorous theory incorporating a full simulation of fluid flow conditions can be developed [4,5]. For measurements made on nuclear power plant internal structure with external detectors a simple phenomenological theory is often necessary and if circumspectly applied, equally valid. A new develop-

ment in this category is the utilization of neutron noise signals [6] to identify the inherent vibrations.

As an example of the rigorous approach, consider the case of the identification of the vibrational behaviour of a cylindrical rod or tube in parallel flow. It is possible to develop a solution, based on exact three dimensional elasticity theory [5] for the cylindrical rod modelled on simple beam theory as

$$(m_r + m_f)\ \frac{\partial^2 v}{\partial t^2} + \bar{E}I\ \frac{\partial^4 y}{\partial x^4} + C\ \frac{\partial y}{\partial t}\ = q(x,t) \qquad \ldots(5)$$

where $q(x,t)$ is the spatially homogeneous and stationary random load field arising from a stationary surface pressure field $p(x,\theta,t)$.

Consider a cylindrical rod or tube bounded by a cylindrical surface S and ends E, subjected to purely normal pressure fluctuations over S. The boundary conditions on E, in cylindrical conditions, are $u_r = u_\theta = \sigma_{zz} = 0$. Then for a linear system

$$\phi(\bar{r}_1,\ \omega_1,\ \bar{r}_2,\ \omega_2)$$

$$= \oint_S \oint_S \phi_p\ (S_1,\ \omega_1,\ \bar{S}_2,\ \omega_2) H_k(\bar{r}_1,\ \bar{S}_1,\ \omega_1) H_K^*(\bar{r}_2,\ \bar{S}_2,\ \omega_2) dS_1\ dS_2 \qquad \ldots(6)$$

where $\phi_p(\bar{S}_1,\omega_1,\bar{S}_2,\omega_2)$ is the cross-spectral density of the surface pressure $p(\bar{S},t)$ acting on S and $\phi_k(\bar{r}_1,\omega_1,\bar{r}_2,\omega_2)$ is the cross-spectral density of the response R_k of type k at any two points $\bar{r}_1$, $\bar{r}_2$. Also $H_k(\bar{r},\bar{S},\omega)$ is the frequency response Green's function defined by

$$H_k(\bar{r},\bar{S},\omega)\ = \int_0^\infty e^{i\omega t}\ h_k(\bar{r},\bar{S},t)\ dt \qquad \ldots(7)$$

in terms of the real time weighting function $h_k(\bar{r},\bar{S},t)$ defined by

$$R_k(\bar{r},t) = \oint_S \int_0^t p(\bar{S},\tau) h_k(\bar{r},\bar{S},t-\tau)\ d\tau dS \qquad \ldots(8)$$

In particular the spectral density at $\bar{r}$ is

$$\phi_k(\bar{r},\omega)\ = \oint_S \oint_S \phi_p(\bar{S}_1,\bar{S}_2,\omega)\ H_k(\bar{r},\bar{S}_1,\omega)\ H_k^*(\bar{r},\bar{S}_2,\omega)\ dS_1\ dS_2 \qquad \ldots(9)$$

The responses of interest refer to the surface r=a and the problem reduces to the calculation of the three frequency response functions $H_k(a,\theta,\ Z,\theta_1,Z_1,\omega)$ where $k = r,\theta,\Sigma$ referring respectively to radial surface displacement u_r, tangential surface displacement u_θ and the surface axial strain differential $\Delta\Sigma_{zz} = \Sigma_{zz}(\theta) - \Sigma_{zz}(\theta+\pi)$. A degree of correlation has been shown to exist between the theoretical predictions of this model and experimental tests (Figure 4) carried out on a HIFAR fuel element liner in a water tunnel.

As shown by Thie (6) it is possible to utilize neutron noise and accelerometer signals to investigate and interpret gross core absorber and fuel movement with respect to the nuclear plant supports without a complete knowledge of the hydraulic forcing functions. A simple equation of harmonic motion with approximate parameters for heavy water can be used to confirm control system resonances and their influence on reactor power and reactivity. The relationship between vibration and reactivity is expressed as an in-core neutron detector fractional noise spectrum

$$\left|\frac{i(j\omega)}{\bar{i}}\right|^2 = \left|\Sigma\left\{\kappa\ (j\omega)\left[\frac{d\rho}{dx}\right]_g + \left[\frac{d\ell n\phi}{dx}\right]_g\right\} x_g(j\omega) + \Sigma\ \kappa(j\omega)\rho_g(j\omega)\right|^2 \qquad \ldots\ (10)$$

where $\kappa(j\omega)$ is the local reactor transfer function, x_g are various components of motion arising from appropriate pressure forces F_g, and ϕ and ϕ are flux and reactivity respectively. Equation(10) can then be used to relate both the amplitude and phase of vibration induced cross-power spectral density peaks to the structure of the normalized reactor transfer function - Figure 3 - as measured by neutron noise analysis.

The use of a relationship such as (10), whilst somewhat empirical and speculative gives a degree of confidence to the visual interpretation of on-line computer displays. The detection of internal malfunctions through the use of a dedicated, medium sized digital computer which also provides emergency shut-down control capability is an attractive if somewhat expensive end point of reactor noise technology. A simple and cheaper interim approach, utilizing the zero crossing or two-state correlation technique (7), could be developed to provide monitoring and control functions without visual display.

5. Summary and Conclusions

Stochastic identification techniques coupled with on-line computer pattern recognition and graphic display facilities will undoubtedly play an important role in ensuring the structural integrity of nuclear power plant in the future. Correlations between vibrational phenomena and stochastic variates such as neutron density and temperature will make possible a range of recording, identification and safety procedures.

Acknowledgements

The author gratefully acknowledges profitable discussion with Professors J.J. Thompson and Z.J. Holy, of the School of Nuclear Engineering, and members of the staff of the Australian Atomic Energy Commission, in particular Mr. Norman Parsons and Dr. R.W. Harris. Financial assistance for the project is being provided by the Australian Institute of Nuclear Science and Engineering.

References

(1) Wax, N. (Editor) Selected papers on noise and stochastic processes, Dover, 1954.

(2) Astrom, K.J. Introduction to stochastic control theory Academic Press, 1970

(3) Harris R.W. The measurement of mechanical integrity in a reactor fuel element by the analysis of external vibration signals, Nuclear Engineering and Design 23, (1972), pp 182-186.

(4) Chen, S.S. and Wambsganns, M.W., Response of a flexible rod to near-field flow noise (1970), pp 5-31.

(5) Thompson, J.J. and Holy Z.J. Random pressure induced vibration of pin ended cylindrical rods, Second International Conference on Structural Mechanics in Reactor Technology. paper D3/6, (1973), Berlin.

(6) Thie, J.A. Theoretical Considerations and their application to experimental data in the determination of reactor internals motion from stochastic signals, paper given at "SMORN 1" Conference, Rome, Italy, 21-25 October 1974.

(7) Uhrig, R.E. (Editor) U.S. Atomic Energy Commission - AEC Symposium Series No.4. Noise analysis in nuclear systems; Proceedings of a Symposium held at the University of Florida 4-6 November 1963, paper by L.G. Kemeny and W. Murgatroyd.

APPENDICES

1. General Langevin Model

Following Wang and Uhlenbeck (Wax, 1954) the complex dynamic system can be represented by:

$$\begin{aligned} Z_{11}y_1 + Z_{12}y_2 + \ldots Z_{1n}y_n &= f_1(t) \\ Z_{21}y_1 + Z_{22}y_2 + \ldots Z_{2n}y_n &= f_2(t) \\ &\vdots \\ Z_{n1}y_1 + Z_{n2}y_2 + \ldots Z_{nn}y_n &= f_n(t) \end{aligned} \qquad \ldots(A1)$$

where

Z_{ik} Linear differential operators of arbitrary order with constant coefficients

y_i "n" time dependent functions representing "n" macroscopic variables defining dynamic behaviour of system

$f_n(t)$ "n" functions representing noise sources arising in each loop of reactor.

Now, according to Wang & Uhlenbeck,

$$|Z||y| = |f| \qquad \ldots(A2)$$

where

$|Z|$ is 'n' by 'n' matrix whose elements are 'n' x 'n' operators in (1)

$|y|$ column matrix with elements functions $y_i(t)$

$|f|$ column matrix with elements functions $f_i(t)$.

Next we define a noise correlation matrix $|\rho|$ with elements

$$\rho_{ij}(\tau) = \lim_{T \to \infty} \frac{1}{2T} \int_{-T}^{T} dt\, y_i(t)y_j(t+\tau) \qquad i,j = 1,2 \ldots n \qquad \ldots(A3)$$

and a fluctuation correlation matrix

$$\phi_{ij}(\tau) = \lim_{T \to \infty} \frac{1}{2T} \int_{-T}^{T} dt\, f_i(t)f_j(t+\tau) \qquad i,j = 1,2 \ldots n \qquad \ldots(A4)$$

as well as their transforms

NOISE SPECTRAL DENSITY MATRIX $|R|$ WITH ELEMENTS $R_{kj}(\omega) = \int_{-\infty}^{\infty} \phi_{kj}(\tau)e^{-2\pi i\omega\tau}d\tau \qquad k,j = 1,2 \ldots n$

FLUCTUATION SPECTRAL DENSITY MATRIX $|F|$ WITH ELEMENTS $F_{kj}(\omega) = \int_{-\infty}^{\infty} \rho_{kj}(\tau)e^{2\pi i\omega\tau}\, d\tau \qquad k,j = 1,2 \ldots n \qquad \ldots(A5)$

2. Identification Algorithm

For identification purposes, if an impulse response g(t) is first calculated from an experimental time series measurement, then a desired, optimal response $h(\alpha;t)$ can be obtained by minimizing the functional

$$\xi = \int_0^T \{\langle\psi|g(t) - h(\alpha;t)|^2\rangle dt \qquad \ldots(A6)$$

where α is a vector of unknown parameters and ψ is an arbitrary weighting vector representing the importance of each component of h and g. A possible optimization scheme will then be to vary the parameters α, a process equivalent to a Gauss Seidel iteration scheme for solving the set of linear equations

$$\frac{\partial\xi}{\partial\alpha_i} = 0 \quad (i = 1,2 \ldots j) \qquad \ldots(A7)$$

3. Time Series Algorithms

In order to synthesize the elements of the correlation and spectral density matrices defined in Appendix 1 from experimental data, time series analysis identification techniques have to be utilized.

The basic algorithms for time-series analysis are given below. Consider two or more time-series

$$x_0 y_0 x_1 y_1 \quad \cdots \quad x_{n-1} y_{n-1}$$

then the following statistical expressions may be computed in order to evaluate the dynamic parameters of a system - such as a nuclear reactor - and to gain an insight into the physical processes which are taking place therein.

Mean Values

$$X = (1/n) \sum x \qquad \ldots(A8)$$

$$Y = (1/n \sum y \qquad \ldots(A9)$$

Variances

If each value of x and y is replaced by

$$\underline{x} = x - X \quad \underline{y} = y - Y$$

then the variances are given by

$$Var_{xx} = \frac{1}{n-1} \sum \underline{x}^2 \qquad \ldots(A10)$$

$$Var_{yy} = \frac{1}{n-1} \sum \underline{y}^2 \qquad \ldots(A11)$$

$$Var_{xy} = \frac{1}{n-1} \sum \underline{x}\,\underline{y} \qquad \ldots(A12)$$

Normalised Auto- and Cross-Covariances

For a lag number s these are given by

$$\psi_{xx}(s) = |(n-s-1)Var_{xx}|^{-1} \sum_{r=0}^{n-s-1} \underline{x}_{r+s} \cdot \underline{x}_r \qquad \ldots(A13)$$

$$\psi_{yy}(s) = |(n-s-1)Var_{yy}|^{-1} \sum_{r=0}^{n-s-1} \underline{y}_{r+s} \cdot \underline{y}_r \qquad \ldots(A14)$$

$$\psi_{xy}(s) = |(n-s-1)\sqrt{Var_{xx} Var_{yy}}|^{-1} \sum_{r=0}^{n-s-1} \underline{x}_{r+a} \cdot \underline{y}_r \qquad \ldots(A15)$$

$$\psi_{yx}(s) = |(n-s-1)\sqrt{Var_{xx} Var_{yy}}|^{-1} \sum_{r=0}^{n-s-1} \underline{y}_{r+a} \cdot \underline{x}_r$$

Auto Spectra

If S is the largest lag and $\overline{\sum}$ means the sum with the first and last terms halved and s is the harmonic number, then

$$W_{xx}(s) = (1/4)w_{xx}(s-1) + (1/2)w_{xx}(s) + (1/4)w_{xx}(s+1) \quad \text{for } s \neq 0 \qquad \ldots(A16)$$

and

$$W_{xx}(0) = (1/2)w_{xx}(0) + (1/2)w_{xx}(1) \qquad \ldots(A17)$$

where

$$w_{xx}(s) = 4V_{xx} \overline{\sum_{r=0}^{s}} xx(\tau).\cos(\frac{rs\pi}{S}) \qquad \ldots(A18)$$

Co and Quad Spectrum

The cross spectrum is defined as the complex quantity $W_{xy} + i\, W_{xy}^*$. These quantities are computed as follows:

$$G_{xy}(s) = (1/4)g_{xy}(s-1) + (1/2)g_{xy}(s) + (1/4)g_{xy}(s+1) \quad \text{for } s \neq 0 \qquad \ldots(A19)$$

and

$$G_{xy}(0) = (1/2)g_{xy}(0) + (1/2)g_{xy}(1) \qquad \ldots(A20)$$

where

$$g_{xy}(s) = 4\sqrt{Var_{xx}Var_{yy}} \sum_{r=0}^{S} (1/2)|\psi_{xy}(r) + \psi_{yx}(r)|.\cos(\tfrac{rs\pi}{S}) \qquad \ldots(A21)$$

and

$$g_{xy}^{*}(s) = 4\sqrt{Var_{xx}Var_{yy}} \sum_{r=0}^{S} (1/2)|\psi_{xy}(r) - \psi_{yx}(r)|.\sin(\tfrac{rs\pi}{S}) \qquad \ldots(A22)$$

from which $G_{xy}^{*}(s)$ can be defined similarly to eqs.(13) and (14). Finally, corrections for the time delay are applied to give

$$W_{xy}(s) = G_{xy}(s)\cos(\tfrac{1}{2}ps) + G_{xy}^{*}(s)\sin(\tfrac{1}{2}ps) \qquad \ldots(A23)$$

and

$$W_{xy}^{*}(s) = G_{xy}^{*}(s)\cos(\tfrac{1}{2}ps) - G_{xy}(s)\sin(\tfrac{1}{2}ps) \qquad \ldots(A24)$$

where $p = \pi/S$.

Phase Lag

This is computed from

$$\phi = \arctan(W_{xy}^{*}/W_{xy}) \qquad \ldots(A25)$$

Coherence Function

This is defined by

$$\zeta = \frac{W_{xy}^{2} + W_{xy}^{*2}}{W_{xx}\,W_{yy}} \qquad \ldots(A26)$$

For purposes of data analysis and stochastic modelling facilities exist for the scanning of up to twenty channels of transducer signals and the multiple cross-correlation of eight data channels. It is planned to interface many of these channels to the HIFAR reactor on a long term basis so that fluctuation phenomena and vibration patterns can be monitored on a routine basis.

4. PREDICTION AND FILTERING TECHNIQUES

Whilst the Wiener and Kalman filters are receiving increasing attention as predictors in control theory, it is useful to trace the development of time domain predictors directly from the basis of time series analysis. We seek to synthesize a time variant linear filter whose output $y(t)$ at any time t is an estimate of the input at a later time $t+\tau$. Thus if $x(t)$ is a typical member of a non-stationary statistical process, we require the filter to minimize the mean square error $[\xi^2(t)]$ between the output $y(t)$ and the input $x(t+\tau)$ at time $t+\tau$.

For an error $\xi(t)$ at time t, we have

$$\xi(t) = y(t) - x(t+\tau) \qquad \ldots(A27)$$

from which we derive the mean square error

$$[\xi^2(t)] = [y^2(t)] - [2y(t)x(t+\tau)] + [x^2(t+\tau)] \qquad \ldots(A28)$$

Assuming that $h(t\alpha)$ is the output of the filter at time t due to a delta function input at time α, then the output $y(t)$ due to the input $x(t)$ is given by

$$y(t) = \int_{0}^{t} h(t,\alpha)x(\alpha)d\alpha \qquad \ldots(A29)$$

Rearranging and combining (A32) and (A33) gives

$$\xi^2(t) = \int_{0}^{t}\int_{0}^{t} h(t,\alpha)h(t,\alpha')\psi(\alpha,\alpha')d\alpha\, d\alpha' - 2\int_{0}^{t} h(t,\alpha)\psi(t+\tau,\alpha)d\alpha + \psi(t+\tau,t+\tau) \qquad \ldots(A30)$$

where $\psi(\alpha,\alpha')$ represents the autocorrelation function of the process

$$\psi(\alpha,\alpha') = [x(\alpha)x(\alpha')] \qquad \ldots(A31)$$

If we now vary the impulse response function $h(t,\alpha)$ by $\delta h(t,\alpha)$ then the first order corresponding variation in $[\xi^2(t)]$ is given by

$$[\delta\xi^2(t)] = 2\int_0^t \delta h(t,\alpha)\left\{\int_0^t \psi(\alpha,\alpha')h(t,\alpha')d\alpha' - \psi(t+t,\tau\alpha)\right\} d\alpha \qquad \ldots(A32)$$

If $h(t,\alpha)$ is the impulse response function of the optimum filter which minimizes $[\xi^2(t)]$, then the variation $[\delta\xi^2(t)]$ vanishes for all $\delta h(t,\alpha)$. Thus we have

$$\int_0^t \psi(\alpha,\alpha')h(t,\alpha')d\alpha' = \psi(t+\tau,\alpha) \quad \text{for} \quad 0 < \alpha < t \qquad \ldots(A33)$$

The equation above can be recognised as a modified Wiener-Hopf integral equation. The solution $h(t,\alpha)$ is the impulse response of the optimum Wiener filter and the resulting mean square error is given by

$$[\xi^2(t)]_{min} = \psi(t+\tau,t+\tau) - \int_0^t h(t,\alpha)\psi(t+\tau,h)dh \qquad \ldots(A34)$$

In the above equation $(t+\tau,t+\tau)$ is the mean power at time $t+\tau$ and the integral on the right hand side represents the maximum difference between the mean power and the mean square error that can be obtained by linear filtering. The auto-correlation function $\psi(\alpha,\alpha')$ uniquely specifies the impulse response function $h(t,\alpha)$ of the Wiener filter.

In order to be able to apply this predictor in time series analysis, we must be able to construct a representative auto-correlation function from a set of sample functions of the process $x_n(t)$ thus

$$\psi(\alpha,\alpha') = \frac{1}{N}\sum_{n=1}^{N} x_n(\alpha)x_n(\alpha') \qquad \ldots(A35)$$

Ideally, the set $x_n(t)$ is determined by performing N sets of measurements under similar conditions. Alternatively the sample functions may be represented by their characteristic modes which must be mathematically determined.

It is likely that, at some future time, system vibrations and abnormal transients in nuclear power plant will be monitored and controlled with safety circuits incorporating optimal predictors.

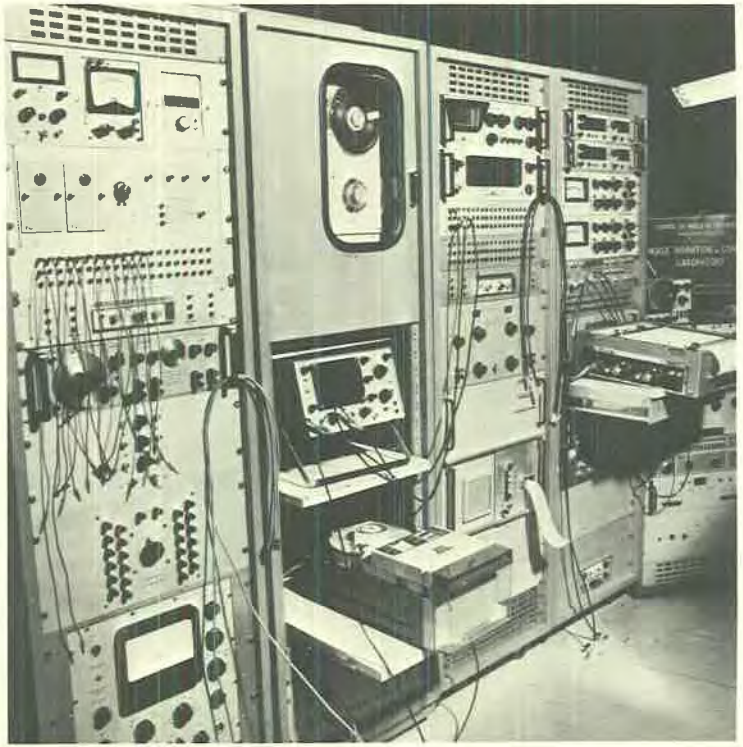

Fig. 1: "SNEDAC" DATA ACQUISITION COMPUTER AND CORRELATOR

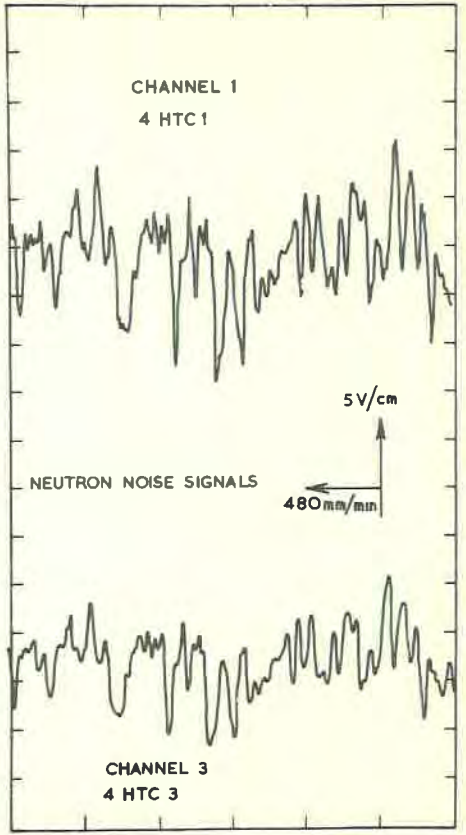

Fig. 2: "HIFAR" NEUTRON NOISE FIELD AND BASIS FOR CROSS-CORRELATION MEASUREMENTS ("HIFAR" is an 11 Megawatt heavy-water research reactor with annular plate type fuel elements)

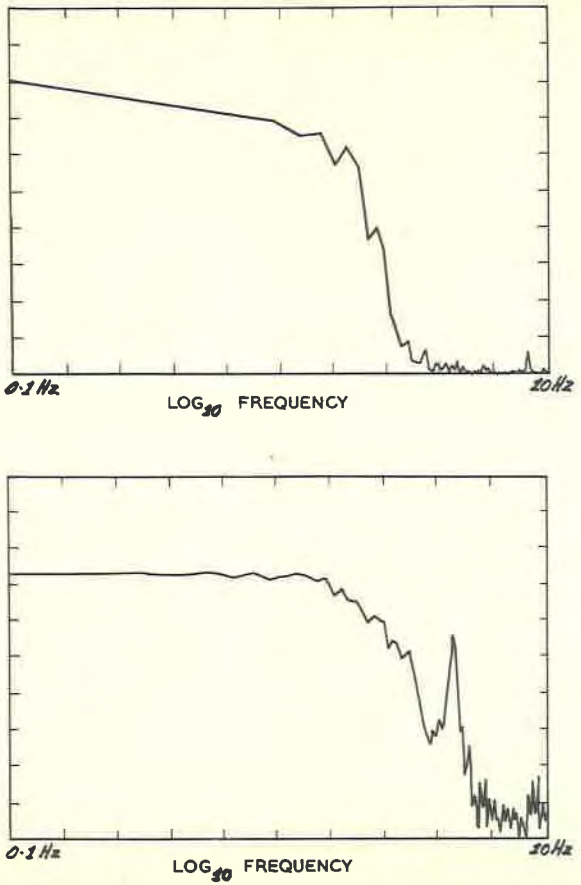

Fig. 3: "HIFAR" TRANSFER FUNCTION AT 5000 WATTS (TOP) AND 100,000 WATTS (BOTTOM) SHOWING INFLUENCE OF CONTROL ARM VIBRATION

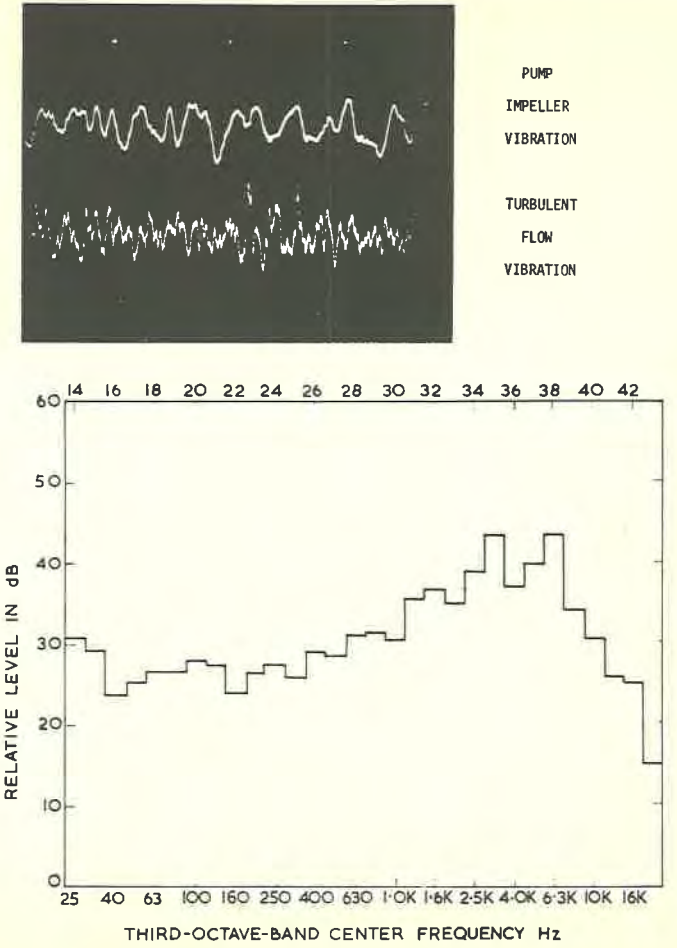

Fig. 4: HYDROELASTIC VIBRATION OF FUEL ELEMENT SHOWING FAR AND NEAR FIELD EFFECTS

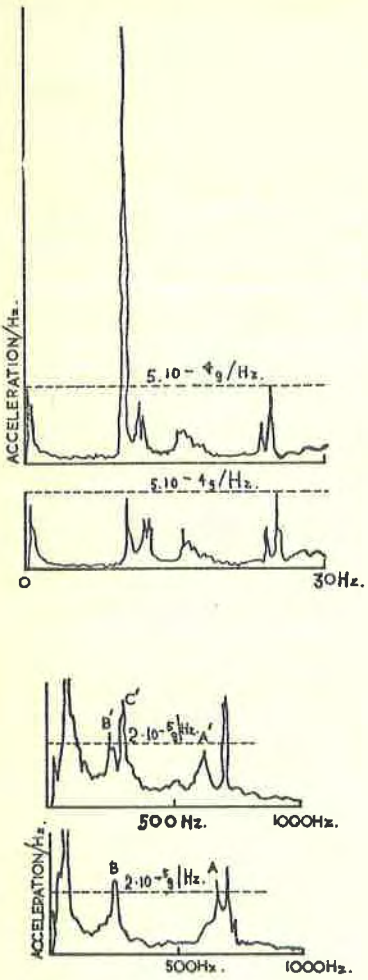

Fuel Elements	Centre	Side
A1	4.5	3.5
A2	8.5	3.5
A3	3.7	2.5
A4	7.0	3.5
B1	7.0	3.0
B2	4.0	2.0
B3	3.0	1.0
B4	6.0	3.0
B5	4.5	2.5
B6	5.0	3.0
C1	5.0	2.5
C2	4.5	2.5
C4	5.0	2.0
C5	6.0	4.0
D1	4.0	1.5
D2	5.0	3.0
D3	4.5	1.0
D4	6.5	1.5
D5	3.5	3.0
D6	3.0	2.5
E1	3.5	2.5
E2	3.5	3.0
E3	2.0	1.5
E4	4.5	2.5

Other Parts of Structure	
CCA2	3.0
CCA5	1.8
4V5	2.7
SR1	2.0

Heavy water weir overflow valve — 12

Fig. 5: ACCELEROMETER SCANNING OF FUEL ELEMENT STRUCTURAL INTEGRITY
(Top left Increase in low frequency resonant peak of dummy fuel element due to enlarged end clearances.
Bottom left Changes in high frequency resonant structure associated with wear of fuel plate supports.
Right Hydroelastic acceleration intensities acting on fuel element matrix and related core components.)